HIGH-POWER TEST OF THE S-BAND ACCELERATOR GUIDE FOR THE KEKB INJECTOR LINAC

S. Yamaguchi, Y. Igarashi*, K. Kakihara and A. Enomoto, KEK, 1-1 Oho, Tsukuba, Ibaraki, 305-0801 Japan, * Mitsubishi Heavy Industries, Ltd., Nagoya Aerospace Systems, Oye 10, Minato, Nagoya, Aichi, 455-0024, Japan

Abstract

A high-power test of an accelerator guide (S-band, 2m-long, quasi-constant gradient, made by electroforming) for an energy upgrade of the KEKB injector linac [1] was performed. An average accelerating electric field of 36 MV/m was achieved for 50-Hz pulses from a SLED. The dark current caused by field-emitted electrons was measured as an index of progress of rf conditioning of the accelerator guide. The obtained field-enhancement factor from modified Fowler-Nordheim plots of the dark current converged to about 70 after rf conditioning for 250 hours. In order to obtain information about rf breakdown, radiation (neutron as well as gamma-rays) emitted from the accelerator guide was measured by a NE213 liquid-scintillation counter.

1 HIGH-POWER TEST

In the usual operation of the linac, the klystron output power (41 MW, 4μs and 50 Hz) is pulse-compressed by the SLED and fed into four 2-m accelerator sections. However, all of the power was fed into one accelerator section in this high-power test. A schematic layout of the experimental setup is shown in Figure 1. The maximum klystron output power and the electric-field strength in the

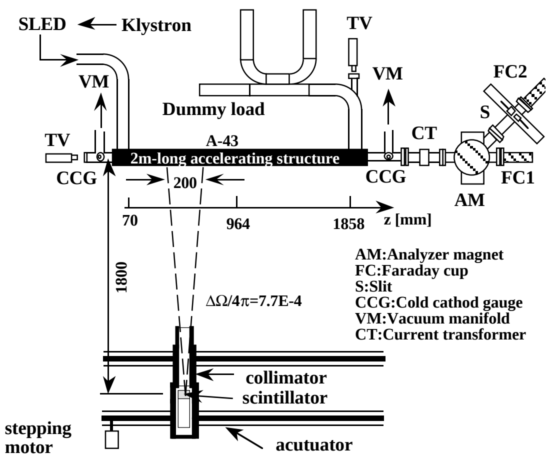

Figure 1: Schematic layout of the experimental setup.

accelerator guide averaged over the pulse were 30 MW and 36 MV/m, respectively, which shows a large margin for the KEKB operation (10.5 MW, 21 MV/m, respectively).

2 MEASUREMENT OF DARK CURRENT

The total amount of the dark current (I) was measured by a Faraday cup 1 (FC1 in Figure 1). The SLED was detuned during the measurement. The measured result is shown in Figure 2 as a modified Fowler-Nordheim (F. N.)

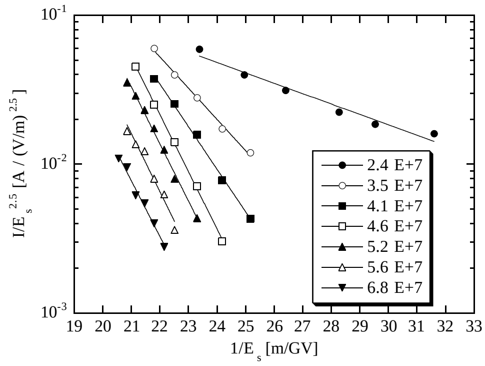

Figure 2: Modified Fowler-Nordheim plot. Numerical values show the number of shots from the start of rf conditioning. E_S(maximum surface field at disk edge) = E_{acc} (accelerating field) $\times$ 2.1.

plot [2]. The field-enhancement factor (β), which can be obtained from the gradient of the F. N. plot, is shown in Figure 3 together with the amount of dark current (I), for an electric field of 21 MV/m. We can see from this figure that while the β value converged to 70 at 4.5x10^7 shots (250 hours at 50 Hz), I continued to decrease after this time and converged at 7$\times$$10^7$ shots (400 hours).

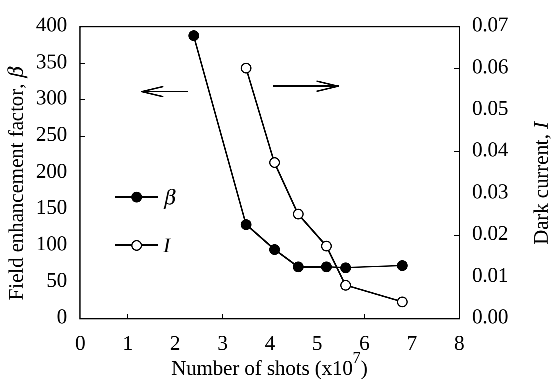

Figure 3: History of the field-enhancement factor (β)and the amount of dark current (I) for E_{acc}=21 MV/m.

Figure 4 shows the momentum spectra of the dark current measured by the analyzer magnet (AM) and

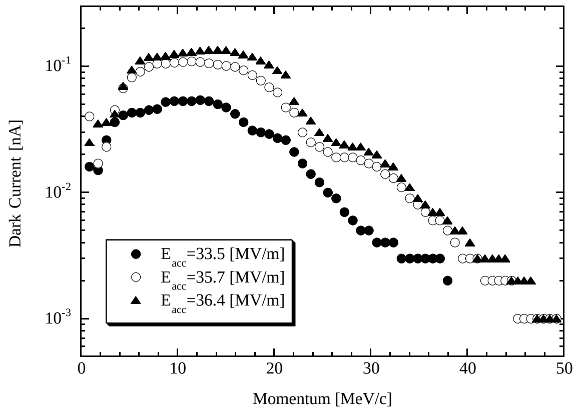

Figure 4: Momentum spectra of the dark current for an average electric field strength of 33.5, 35.7, 36.4 MV/m.

Faraday cup 2 (FC2). It is observed that the peak energy is much lower than the accelerating energy (about 70 MeV), calculated from accelerating gradient and structure length.

3 MEASUREMENT OF RADIATION

In order to obtain information about rf breakdown, radiation (neutrons as well as γ-rays) emitted from the accelerator guide was measured with a NE213 liquid-scintillation counter (51 mm in diam. by 51 mm in height) using a pulse-shape discrimination technique. A schematic diagram of the electronic circuit is shown in Figure 5.

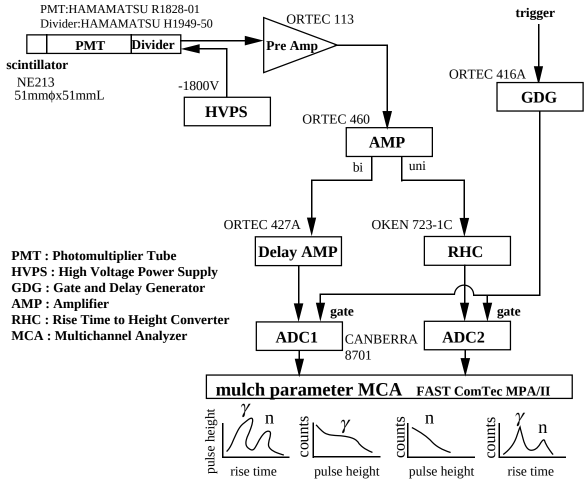

Figure 5: Schematic diagram of the electronic circuit.

We first, examined the dependency of the count rate of radiation on the gate width (t_W) and gate delay (t_d) time. Figure 6 shows the relation between the rf pulse and gate signal width and delay. It is shown in Fig. 7 that radiation (both γ-rays and neutrons) is uniformly emitted during a pulse at the location z = 964 mm; however, at z = 1858 mm (near output coupler) and t_W = 1μs, neutrons

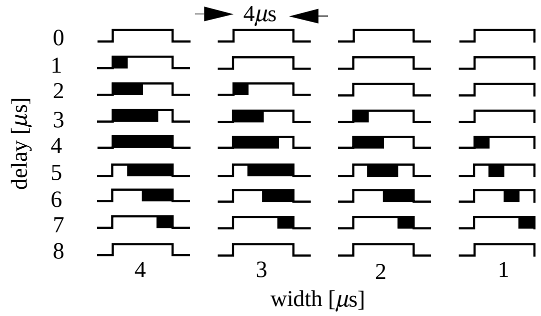

Figure 6: Relation between the rf pulse and gate signal. The gate is open for the black area.

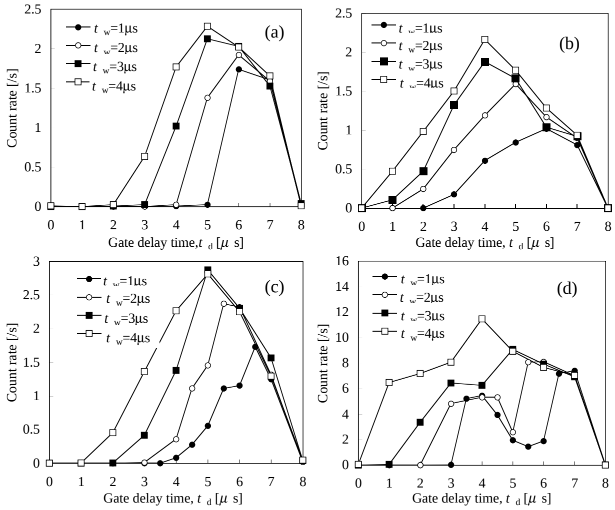

Figure 7: Count rate of radiation for various vs. gate delay for various gate widths and locations. (a) z=964, γ-rays, (b) z=964, neutrons, (c) z=1858, γ-rays, (d) z=1858, neutrons.

at the pulse's edge are five-times more than that at the middle region of the pulse. This fact suggests that rf breakdown can easily occur at a pulse's edge. In the measurement mentioned below, t_W and t_d were fixed as 4μs.

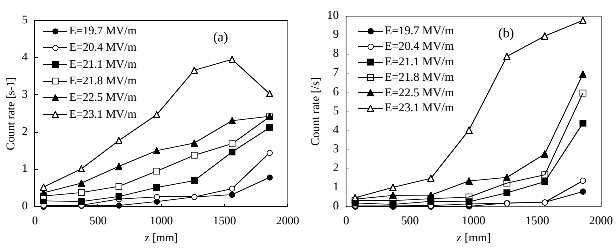

Figure 8: Dependence of the count rate on the detector position. (a) γ-rays, (b) neutrons.

Figure 8 shows the dependence of the count rate of radiation on the detector position. A glance at the figure reveals that the count rate increases exponentially, except for at E = 23.1 MV/m.

The graph in Figure 9 illustrates the dependence of the count rate of radiation on the electric-field strength. It is shown that the count rate of γ-rays increases exponentially; however, neutrons suddenly increase at the output coupler, except for at z = 1858 mm.

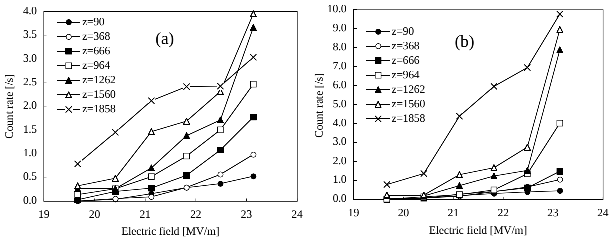

Figure 9: Dependence of the count rate on the electric-field strength. (a) γ-rays, (b) neutrons.

Energy spectra of the γ-rays and neutrons were obtained by unfolding the pulse-height spectra. Response matrices of γ-rays and neutrons were calculated by EGS4 [3] and SCINFUL [4] code, respectively (see, Figure 10). The energy

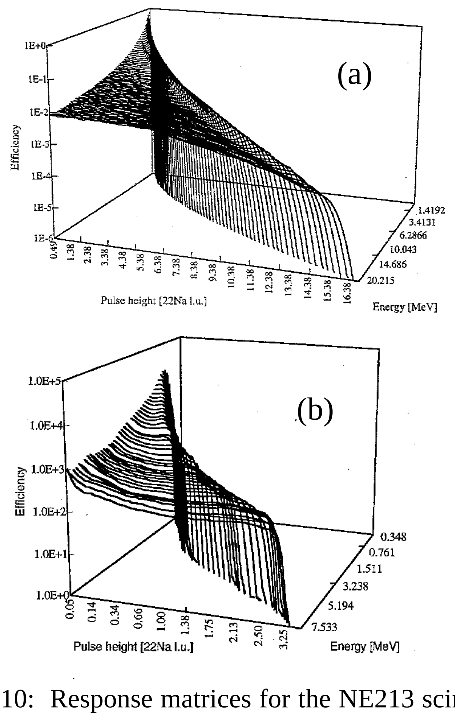

Figure 10: Response matrices for the NE213 scintillator. (a) γ-rays, (b) neutrons.

resolution of the detector for γ-rays and neutrons was determined by comparing the measured pulse-height spectra for standard γ-ray sources and the calculated ones by EGS4.

Figure 11 shows the energy spectra unfolded using the FORIST code [5] for z=1858 mm (near output coupler). The γ-ray energy is fairly low (the flux has a maximum at energy of 1.5 MeV). It is likely that this is due to the fact that the γ-rays have strong anisotropy and

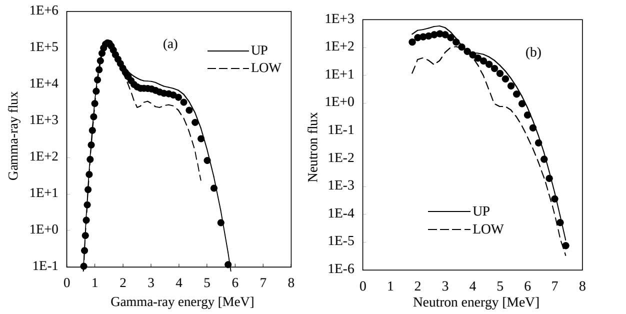

Figure 11: Energy spectra for z=1858 mm. (a) γ-rays, (b) neutrons.

the low-energy component is dominant in the direction of 90 degree, where the detector has been set. It is reasonable to think that the neutrons are generated by a giant resonance reaction of copper nuclei based on the facts that the peak energy of neutrons is a few MeV (Fig. 11) and the peak energy of field-emitted electrons is around 10 MeV (Fig.4). Also, the reaction cross section of the giant resonance has a maximum at 10 to 20 MeV.

5 CONCLUSIONS

An accelerating gradient of 36 MV/m (4μs, 50 Hz, averaged over SLED pulse) was obtained for an accelerator guide for the KEKB injector linac. The field-enhancement factor (β) obtained from a modified Fowler-Nordheim plot converged to 70 after 250 hours of conditioning. From a measurement of the optical neutrons, it has been revealed that the neutron are emitted in large quantities at the rf pulse's edge, which suggests that rf breakdown can easily occur at that time.

6 ACKNOWLEDGMENTS

The authors wish to acknowledge valuable discussions concerning a high-power test of the accelerator guide with T. Higo. They wish to thank Y. Namito for his valuable comment on the angular distribution of the optical neutrons. We also acknowledge F. Maekawa for supplying the FORIST code. The SCINFUL code is provided by NEA data bank.

7 REFERENCES

[1] A. Enomoto: 'Construction Status of the KEKB 8-GeV Injector Linac', these proceedings.

[2] G. A. Loew and J. W. Wang: 'RF Breakdown Studies in Room Temperature Electron Linac Structures', SLAC-PUB-4647 (1988).

[3] W. R. Nelson, H. Hirayama and D. W. O. Rogers: 'The EGS4 Code System', SLAC-265 (1985).

[4] J. K. Dickens: 'A Monte Carlo Based Computer Program to Determine a Scintillator Full Energy Response to Neutron Detector for E_n Between 0.1 and 80 MeV:User's Manual and FORTRAN Program Listing', ORNL-6462 (1988).

[5] R. H. Johnson: 'FORIST:Neutron Spectrum Unfolding Code - Iterative Smoothing Technique', PSR-92, ORNL/RSIC (1975).